



Rheological characterization of SCC mortars and pastes with changes induced by cement delivery

Sandra Nunes^{a,*}, Paula Milheiro Oliveira^b, Joana Sousa Coutinho^a, Joaquim Figueiras^a

^a LABEST/FEUP, Department of Civil Engineering, University of Porto, Portugal

^b CEC/FEUP, Department of Civil Engineering, University of Porto, Portugal

ARTICLE INFO

Article history:

Received 22 March 2010

Received in revised form 18 September 2010

Accepted 21 September 2010

Available online 18 October 2010

Keywords:

A. Self-compacting concrete (SCC)

Cement variations

Mortar

Paste

Rheology

Superplasticizers

Interaction

ABSTRACT

The present paper deals with the influence of different date produced cement on the rheological properties of SCC mortar/paste mixes. Twelve reference SCC mortar/paste mixes (corresponding to four different types of cement and three different levels of aggregate content) displayed workability variation due to different deliveries of cement, supplied from the same factory. Physical and chemical analysis of cements was carried out for the different deliveries. Mortar and corresponding paste mixes were characterized in fresh, hardening and hardened states. Spearman's correlation coefficient was used to investigate whether there is any kind of association within cement characteristics and between cement characteristics and SCC mortar/paste test results. Existing models for predicting the mini-slump flow diameter and the flow time of pastes were implemented and compared with experimental data. The target paste properties for different fine aggregate content were defined in terms of both empirical test results and rheological parameters, linking mortar and paste properties adequate for SCC.

© 2010 Elsevier Ltd. All rights reserved.

1. Introduction

Rheology of cement paste largely dictates rheology of concrete, given a specific aggregate skeleton [1,2]. The key role of the paste is clearly shown by the strong effect on concrete workability of the powder materials, water/powder ratio and of superplasticizer dosage. Furthermore, important phenomena in fresh concrete, like air entrapment and aggregate segregation are determined from paste rheology (along with the stabilising effect of smaller aggregate particles), which provides more or less freedom of motion to aggregates and air bubbles. In spite of the importance of paste rheology, there is no generally accepted procedure for its study. Therefore, direct comparison between different works and the definition of rheology-based acceptance criteria for SCC paste is often difficult. Ultimately, it would be desirable to predict concrete behaviour from paste characteristics. Tests on paste are easier to carry out and require less material. Although rheological tests require more expensive equipment and specific training, they allow a more fundamental and precise characterization of cement suspensions.

The rheology of a superplasticized cement suspension is mainly controlled by: interparticle interactions and state of flocculation of

particles (mainly determined by type and amount of superplasticizer added, but also mixing power and history); particle packing (determined by particle size distribution); and type and amount of hydration products formed (mainly determined by cement chemistry and fineness but also cement–superplasticizer interaction). The rheology of superplasticized cement paste, mortar or concrete can be affected by various factors [3–6], namely,

- the amount, the chemical composition and the molecular structure of the admixture;
- the chemical composition of cement (especially C_3A content and availability of soluble sulfates during the workable period);
- the specific surface of cement;
- the presence of mineral additions or of other types of admixtures;
- technological aspects such as mixing power and instance of admixture introduction;
- environmental aspects such as humidity and temperature.

It is therefore difficult to ascertain the main factors and interactions existing between the different components in a superplasticized cement suspension which is further complicated by the ongoing hydration reactions of cement.

According to BIBM et al. [7] all cements which conform to EN 197-1:2001 can be used for production of SCC. Generally, cement is seen as one of the constituent materials of concrete with less

* Corresponding author. Address: Departamento de Engenharia Civil, Faculdade de Engenharia da Universidade do Porto, Rua do Dr. Roberto Frias, 4200-465 Porto, Portugal. Tel.: +351 225082121; fax: +351 225081835.

E-mail address: snunes@fe.up.pt (S. Nunes).

variation due to a stringent quality control during production. However, recent studies have shown that cement variations have a greater effect on workability and on early reactions of concrete than is generally thought [8–10]. Kubens and Wallevik [10] found that the effect of the production date of cement on rheology was only slight in mixtures without admixtures but more prominent in mixes containing dispersing admixtures. Yield stress results of blank, polycarboxylate ether and melamine mixes (7 samples), containing CEM I 52.5 R, exhibited coefficients of variation of 15%, 44% and 39%, respectively. A similar trend was observed for mixes containing other cements (three CEM I 42.5 R from different producers, and one CEM II/B-S 32.5 R) [10]. Juvas et al. [8] found similar conclusions when comparing the spread flow results of mortars without admixture, containing a typical melamine plasticizer and a polycarboxylate plasticizer, from 50 samples of daily collected CEM I 52.5 R cement type. Larger variations were observed with mixtures containing admixtures when compared to plain mixtures.

The rheology of plain mortar mixtures, with a water/cement ratio of about 0.50, is controlled largely by water [11]. In these mixtures, the cement grains are not uniformly dispersed throughout the water but tend to form small flocs which trap water within them. By adding water these cement flocs are kept apart influencing the rheology of the paste [11]. Later in time, the first hydration products begin to interfere with the unrestricted movement of the cement flocs. Dispersing admixtures are used to both break up the flocs and to maintain the dispersion in a way that causes the cement particles to distribute more uniformly throughout the aqueous phase, reducing the yield stress value for a given water content and so increasing the fluidity of the mix. Not only has the fluidity increased, but more sites on the surface of the cement grains are available for interaction with superplasticizer and hydration [12]. If water is removed from the system, lowering the water/cement ratio to 0.3–0.4, like in the case of mixtures mentioned above [8–10], the fluidity can be reduced back to what it was before the addition of admixture. However, the average inter-grain distance will also reduce, so less hydration will be necessary before the space between the cement grains is filled with hydration product to give setting and strength development [12]. Finally, there will be less void space, not filled with any hydration product, resulting in fewer capillaries and therefore improved final strength and better durability [12]. In conclusion, the mixtures containing superplasticizers are more complex systems and at low w/c ratios a small difference in the dispersion effect of the admixture changes the fluidity remarkably.

Wallevik et al. [9] reported that the fluctuations observed in mortar, due to cement variations, can also be observed at the concrete level. It is suggested that the influence of cement variations on concrete properties can be more or less pronounced depending on cement content in the concrete mixture [9]. In the case of self-compacting concrete, a high-range water reducer must be incorporated and often mixtures have a higher content of cement when compared to conventional concrete mixtures. For these reasons, cement variations have become an important factor when discussing the robustness of SCC production.

A methodology was developed for the design of mortar mixtures which are adequate for SCC [13]. This methodology was developed in three phases: first, the experimental phase conducted according to a central composite design; second, the statistical analysis and model fitting of data collected during the experimental phase and, third, the numerical optimization of mixture parameters using the models derived in the previous phase. Contour plots and interaction diagrams representing the range of mixture parameters where SCC can be found were obtained for each combination of cement type + mineral addition + superplasticizer [13]. This methodology was used to design the SCC mortar mixes

investigated in the present study. A central composite design (2^4 factorial statistical design augmented with 8 axial runs plus 4 central runs) was used to establish numerical models relating mixture parameters to spread flow (D_{flow}), flow time (T_{funnel}) and compressive strength (at 28 days) of mortar. SCC mortar mix proportions were established based on the following mixture parameters: water to powder volume ratio (V_w/V_p); water to cement weight ratio (w/c); superplasticizer to powder weight ratio (Sp/p); sand to mortar volume ratio (V_s/V_m). The derived numerical models were used to find optimized solutions within the experimental domain, i.e. mixtures which exhibit both a spread flow of 260 mm and a flow time of 10 s, similar to values recommended by Okamura et al. [14].

The three main goals of the current study are: first, to assess how large the fluctuations on fresh mortar/paste properties can become when a new delivery of cement is used; second, to identify the constituents in cement which might have caused the fluctuations in mortar/paste properties and, third, to verify if the different test results obtained on pastes correlate with each other, in particular, empirical and rheological test results. To accomplish this, twelve SCC mortar/paste mixes (corresponding to four different Portland cement types, namely, CEM I 52.5R, CEM I 42.5 R, CEM II/A-L 42.5 R and CEM II/B-L 32.5 N, and three different levels of aggregate content) were characterized in the fresh, hardening and hardened states, for eight cement deliveries with different production dates. These mortars also incorporated limestone filler, CEN standardized sand and a polycarboxylate type superplasticizer. The testing programme included standard tests on cements, physical and chemical analysis of cements, empirical tests on SCC mortar and pastes, rheological tests on SCC pastes, experimental packing density and semi-adiabatic tests on SCC pastes.

2. Experimental programme

2.1. Materials characterization and mix proportions

The mortar and paste mixes investigated in this study were prepared with cement, a mineral addition (limestone filler), reference sand conforming to CEN EN 196-1:2006 and tap water. The chemical and physical properties of the different cement types used (first delivery) and limestone filler are presented in Table 1. The mean particle size of limestone filler was 4.5 μm . A commercially available polycarboxylate type superplasticizer (Sika Viscocrete 3000[®]) was used having a specific gravity of 1.05 and 18.5% solids content. Reference sand was a siliceous round grain natural sand (0.08–2 mm) with a specific gravity of 2.57 and an absorption value of 0.68% by mass.

The mix proportions of mortar and paste, for each cement type, were established based on the mixture parameter values presented in Table 2. Mortar mix proportions were adjusted to attain similar fresh properties (D_{flow} = 260 mm and T_{funnel} = 10 s), for each cement type, in a previous study [13]. As can be observed in Table 2, in mortar mixtures exhibiting the same V_s/V_m and w/c ratios (see cases with V_s/V_m = 0.5 and w/c = 0.45), the Sp/p and V_w/V_p had to be adjusted when changing cement type to attain similar mortar fresh properties. V_w/V_p values did not change significantly but Sp/p varied considerably with cement type.

2.2. Mixing sequence and testing sequence

The mortar and paste mixes were prepared in the laboratory in 1.4 and 1.25 l batches, respectively, and mixed in a two-speed mixer complying to NP EN 196-1:2006. The mixing sequence consisted of mixing sand and powder materials (or only powders, in the case of pastes) with 0.81 of the mixing water during 60 s, stopping the

Table 1

Chemical and physical properties of tested cements (1st delivery) and limestone filler (information provided by the supplier). Mineral composition was measured by XRD/Rietveld method.

	CEM I 52.5R	CEM I 42.5R	CEM II/A-L 42.5R	CEM II/B-L 32.5 N	Limestone filler
C ₃ S (%)	67.5	62	55.6	44.4	–
C ₂ S (%)	7.8	9.6	10.4	6.8	–
C ₄ AF (%)	8.9	9.3	9	6.6	–
C ₃ A (%)	7.6	7.6	6.3	5.6	–
Gypsum (%)	4.0	4.5	5.4	7.2	–
CaCO ₃ (%)	1.9	4.6	10.2	26.3	99.0
Total (%)	97.7	97.6	96.9	96.9	99.0
SiO ₂ (%)	18.71	18.76	17.41	14.35	–
Al ₂ O ₃ (%)	5.47	5.31	5.03	4.2	<0.4
Fe ₂ O ₃ (%)	3.05	3.23	2.98	2.54	0.04
CaO (%)	63.96	63.19	62.26	58.87	–
MgO (%)	1.8	1.71	1.7	1.36	–
SO ₃ (%)	3.25	3.04	2.84	3.27	–
Loss on ignition (%)	1.92	2.72	5.82	12.74	43.10
Total (%)	98.16	97.96	98.04	97.33	–
Na ₂ Oeq. (%)	0.78	0.86	0.75	0.62	–
Free CaO (%)	2.67	1.38	1.15	1.24	–
Specific density (g/cm ³)	3.13	3.16	3.11	3.02	2.70
Blaine (cm ² /g)	3830	3270	3710	4230	5150
Residue, 90 µm (%)	0.0	2.1	1.2	2.6	7.9
Residue, 45 µm (%)	6.9	16.9	16.2	18.4	23.7
Residue, 32 µm (%)	18.7	29.3	29.1	30.2	30.8
Mean size (µm)	15.0	18.10	17.92	17.18	8.21
<i>f</i> _c (MPa) (mortar prisms) 2 days	38.9	31.4	29.3	21.2	–
7 days	54.3	46.9	43.6	32.1	–
28 days	62.7	56.4	52.2	38.3	–
Vicat test					
Initial set (min.)	135	145	150	125	–
Final set (min.)	175	195	195	225	–

mixer to scrape material adhering to the mixing bowl, mixing for another 60 s, adding the rest of the water with the superplasticizer, mixing for 60 s, stopping the mixer again to scrape material adhering to the bowl, mixing for another 30 s, stopping the mixer for 5 min and finally mixing mortar/paste during a further 30 s. The mixer was always set at low speed except in the last 30 s of the mixing sequence where it was set at high speed.

The mortar testing sequence was approximately the following:

- 0 h 00 min – start of mortar mixing procedure;
- 0 h 10 min – start of mortar flow test;

- 0 h 15 min – start of mortar V-funnel test;
- 0 h 17 min – moulding of three 70 mm cubes.

The paste testing sequence was approximately the following:

- 0 h 0 min – start of paste mixing procedure;
- 0 h 10 min – start of Marsh cone flow test;
- 0 h 20 min – start of paste flow test;
- 0 h 25 min – start of semi-adiabatic calorimeter test;
- 0 h 30 min – start of 1st rheological test in the rheometer;
- 0 h 32 min – start of centrifuge test;
- 0 h 40 min – start of 2nd rheological test in the rheometer;
- 0 h 42 min – moulding of three prismatic test specimens (4 × 4 × 16 mm³).

In general, for each cement delivery, SCC mortar and paste characterization tests were carried out in the same day to minimize the influence of environmental factors. During the waiting periods between tests the mortar/paste sample was covered with a damp cloth to avoid the loss of water by evaporation. Just before the beginning of each test the mortar/paste sample was re-mixed by hand with a paddle (10 turns clockwise) to destroy any structure formed during resting (thixotropy effects).

2.3. Mortar test methods

2.3.1. Mortar flow and V-funnel tests

Mortar tests using the flow cone and the V-funnel, with the same internal dimensions as the Japanese equipment, were carried out to characterize the fresh state (see [14] for details on equipment and test procedures). The mortar flow test was used to assess deformability by calculating the flow diameter (*D*_{flow, mortar}) as the mean of two diameters of the spread area. The V-funnel test was used to assess the viscosity and passing ability of the mortar. Test flow time was recorded (*T*_{funnel, mortar}).

2.3.2. Compressive strength at 28 days

After fresh mortar tests, three 70 mm cubes were moulded, without compaction, to evaluate 28 day compressive strength (*f*_{c,28, mortar}). Mortar cubes were demoulded one day after casting and kept inside a chamber under controlled environmental conditions (Temperature = 20 °C and HR = 95–98%) until testing age. Compressive strength at 28 days (*f*_{c,28, mortar}) was taken as the mean compressive strength of the three cubes.

Table 2

Optimized mixture parameters and mix proportions.

Cement type	CEM I 52.5R			CEM I 42.5R			CEM II/A-L 42.5R			CEM II/B-L 32.5 N		
Mix reference	A	B	C	A	B	C	A	B	C	A	B	C
<i>Mixture parameters</i>												
<i>w/c</i>	0.45	0.43	0.41	0.45	0.38	0.36	0.45	0.37	0.33	0.45	0.40	0.35
<i>Sp/p</i> (%)	1.90	1.99	2.05	1.72	1.86	1.89	1.58	1.83	1.89	1.49	1.49	1.41
<i>Vw/Vp</i>	0.724	0.716	0.700	0.728	0.710	0.704	0.719	0.713	0.705	0.725	0.714	0.714
<i>Vs/Vm</i>	0.50	0.49	0.47	0.50	0.45	0.43	0.50	0.45	0.40	0.50	0.45	0.40
<i>Mix proportions of mortar (kg/m³)</i>												
Cement	466.5	494.8	532.5	468.3	601.1	654.3	464.6	618.5	751.9	466.9	572.7	714.1
Limestone filler	378.3	373.0	379.3	374.5	346.4	335.0	376.9	323.1	288.8	361.0	349.3	300.3
Water	205.6	207.3	211.3	207.7	221.9	227.8	206.9	222.7	239.1	208.8	225.8	245.3
Superplasticizer	16.1	17.2	18.7	14.5	17.6	18.7	13.3	17.2	19.6	12.4	13.8	14.3
Standardized sand	1286	1260	1209	1286	1157	1106	1286	1157	1029	1286	1157	1029
<i>Mix proportions of paste (kg/m³)</i>												
Cement	932.9	970.1	1004.6	936.6	1092.9	1147.9	929.2	1124.6	1253.2	933.9	1041.3	1190.2
Limestone filler	756.6	731.4	715.6	749.0	629.9	587.6	753.9	587.4	481.3	722.0	635.0	500.5
Water	393.6	389.6	383.2	397.8	389.2	386.5	396.4	390.6	386.9	400.1	396.1	397.1
Superplasticizer	32.1	33.8	35.2	29.0	32.0	32.8	26.6	31.3	32.7	24.7	25.0	23.8

2.4. Paste test methods

2.4.1. Marsh cone flow test

The Marsh cone flow test, including the geometry of testing apparatus, is described in NP EN 445 as a method to determine the fluidity of injection grouts for rocks, soils, or prestressing ducts. This test method is based on the measurement of the time taken for a certain volume of material to flow through the cone. In the present study, 1000 ml of paste was poured into the cone (with an opening of 10 mm in diameter) and the time taken for 500 ml to flow out was taken as the flow time. Paste flow time (T_{flow}) was given by the mean of results obtained in two consecutive measurements. Flow time varies inversely with paste fluidity [15,16].

2.4.2. Paste flow test

The mini-slump flow test was carried out to assess the deformability of paste. A truncated cone (with upper and lower diameters of 19 and 38 mm, respectively, and height of 57 mm) was used in this test, which is a smaller-scale version of the Abrams cone developed by Kantro [15]. After filling the cone with paste and levelling it, the cone was lifted and the paste flow diameter ($D_{\text{flow, paste}}$) was taken as the average of two diameters of the spread area.

2.4.3. Semi-adiabatic calorimeter test

The cement hydration reactions are exothermic. In this study, the heat of reaction of SCC pastes was measured with a simple semi-adiabatic calorimeter specially built for this study (see Fig. 1) based on the calorimeter described in [8]. It consists of a plastic box filled with insulation material forming four cavities in the centre where four cylindrical containers can be fitted. After filling these containers with cement paste, the box was closed. The insulation material surrounding cement samples avoided rapid dissipation of heat to the environment. All tests were carried out in a chamber with controlled environmental conditions (Temperature = 20 ± 2 °C and HR = $50 \pm 5\%$).

The temperature evolution of cement samples was continuously monitored, during 48 h, through the installation of temperature sensors (PT100), outside the bottom part of each container, connected to an automatic acquisition system (datataker DT 515 Series 3) (see Fig. 1). The mean value of three curves of temperature evolution with time was obtained for each cement sample. From this curve three points were selected for our study (see white dots in Fig. 2) and the following data was collected: the initial temperature of paste (Temp. initial); the time to start of temperature raise (Time acceler.); the time to reach maximum temperature (Time peak) and the value of maximum temperature (Temp. peak).

2.4.4. Rheological tests (using a rheometer)

Rheological characterization of cement pastes was carried out focused only on flow behaviour. Yield stress (σ_0) and plastic viscosity (η_{pl}) parameters were determined from the flow curve data by using the Bingham model. According to this model, the relationship between shear stress (σ) and shear rate ($\dot{\gamma}$) is of the form,

$$\sigma = \sigma_0 + \eta_{pl} \dot{\gamma} \quad (1)$$

A rotational rheometer CVO-100 (Bohlin Instruments) was used. Data acquisition and control were performed on a PC-coupled to a CVO-100 rheometer. The measuring device consisted of a cone and plate geometry. The cone diameter was 40 mm with a cone angle of 4°, providing a gap of 150 μm . A viscometry test (shear stepped), in shear rate control mode, was selected to obtain equilibrium flow curves.

Before measurements a pre-conditioning procedure was applied. The temperature was controlled and kept constant at

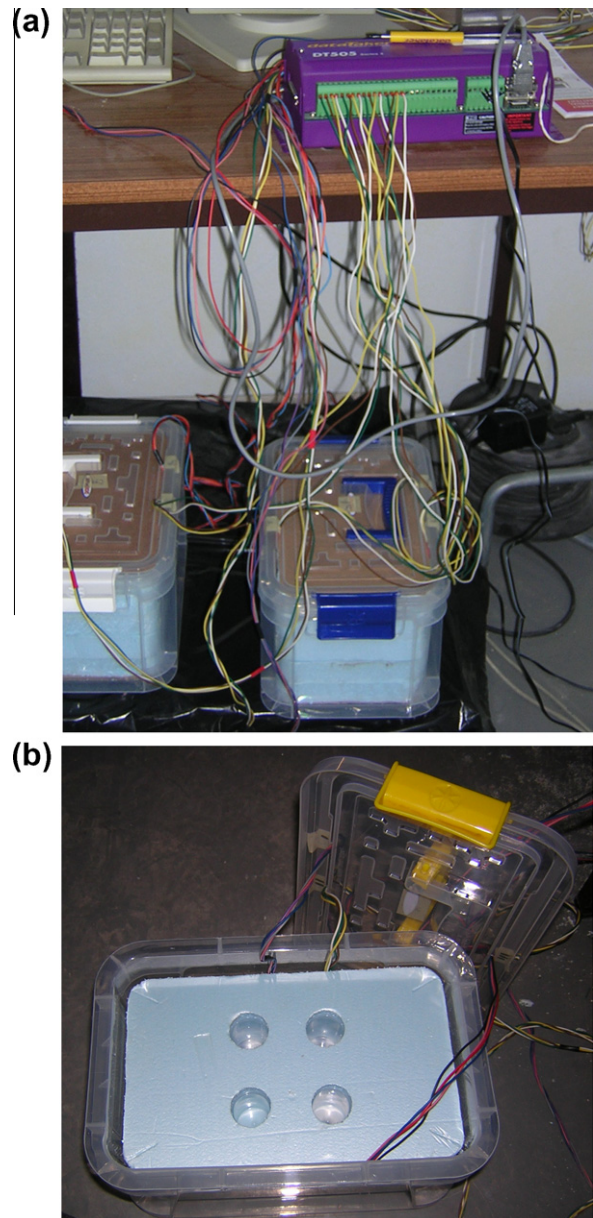


Fig. 1. Experimental set-up used in this study to measure temperature evolution of paste under semi-adiabatic conditions.

25 ± 0.1 °C throughout the testing sequence. A pre-shear was applied to homogenize the sample during 45 s at a shear rate of 200 s^{-1} , followed by a resting period of 100 s (with no shear applied). During the measurements the rheometer was programmed to perform a 12-step logarithmic increase of shear rate ranging from 0.1 to 200 s^{-1} and back again to complete a full cycle. Each measurement consisted of a delay and integration times. The shear rate was applied for the delay time (set equal to 10 s), but no information was recorded during this period. The average value of shear stress was measured for the integration time (set equal to 5 s) and the viscosity was then calculated as the ratio of average shear stress to imposed shear rate.

The descending part of the obtained flow curves were fitted to the Bingham model (see Eq. (1)), as illustrated in Fig. 3. Only data points corresponding to a shear thinning behaviour were used; in some cases the last one or two data points were excluded because the material started to exhibit a shear thickening behaviour for these higher shear rates. The cement paste used as an example in

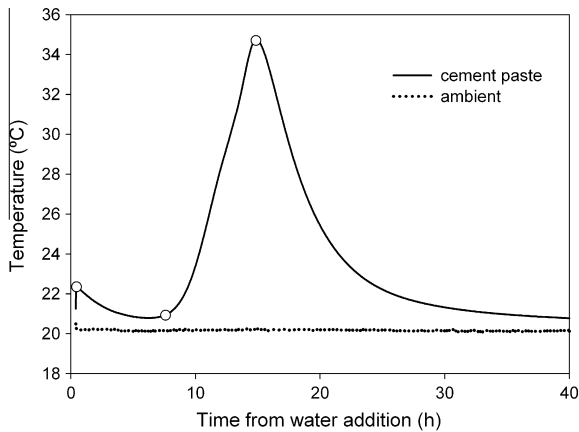


Fig. 2. Typical evolution of temperature of cement paste (SCC) with time obtained from the semi-adiabatic test.

Fig. 3 can be characterized by a yield stress of 1.22 Pa and a plastic viscosity of 0.545 Pa s. The adjusted model parameters, yield stress (σ_0) and plastic viscosity (η_{pl}), were taken as the rheological test results for the present study.

The selected measuring tool (cone and plate; 4°/40 mm), which has the major advantage of imposing a constant shear rate through the sample, may be subject to some criticism. The corresponding gap size is 150 μm , allowing for a maximum 'particle size' of 15 μm , according to [17]. As can be observed in Table 1 the coarser cements have particles with sizes as high as 90 μm . However, the mean particle size of the studied cement pastes was around 15 μm or lower since limestone filler (finer than cement) was added to the mixtures, thus satisfying the requirement established in [18]. Furthermore, a superplasticizer was always included preventing the formation of large flocculates. Concerning the selected rheological model, other authors have suggested more complex models to characterize cement pastes behaviour [19]. In the present study, the Bingham model was selected for its simplicity (a low number of adjustable parameters).

2.4.5. Centrifuge test

A centrifuge (Centurion, model K240 series K2) was used to compact the solids and to determine the free water of the paste, which allowed calculating the packing density of the paste. The free water is defined as the water not restricted by particles, e.g. the water that can move around particles [20]. About 30 min after the beginning of mixing, the four plastic containers (50 ml volume capacity) of the centrifuge were filled with paste (approximately 30 ml on each container). Then, centrifuging was carried out for

15 min at 3500 rpm (relative centrifugal force = 2500 \times g). After that, the free water which rose up to the surface of the paste was removed with a pipette. The weight of the containers before and after centrifuging was determined. The free water content (w_{free}) was calculated from

$$w_{\text{free}} = \frac{w_{\text{initial}} - w_{\text{final}}}{30} \quad (2)$$

where w_{initial} and w_{final} are the weight of containers before and after removing the surplus of water, respectively.

2.4.6. Compressive tests at 28 days

After fresh paste tests, three prismatic moulds ($4 \times 4 \times 16 \text{ mm}^3$) were filled, without compaction, to evaluate 28 day compressive strength. Paste prisms were demoulded one day after casting and kept inside a chamber under controlled environmental conditions (Temperature = 20 °C and HR = 95–98%) until testing age.

2.5. Test results

Workability variations were introduced in twelve reference SCC mortar/paste mixes (see Table 2) due to different deliveries of cement (regularly spaced of about one month, except the first one, as can be observed in Fig. 4). The mortar and corresponding paste mixes were characterized in the fresh, hardening and hardened states and their results are presented in Tables 3–6. The only parameter changing was cement depending on delivery. By using the quality controlled CEN sand, effects on mortar rheology resulting from the sand were reduced to a minimum.

3. Discussion of results

In the first part of this section, only mix A results, all exhibiting the same $V_s/V_m = 0.5$ and $w/c = 0.45$ (see Table 2) will be analysed to assess the effect of cement delivery on fresh mortar/paste properties. In the second part, all paste test results of mixes A–C are used to verify if the different test results obtained on pastes correlate with each other, in particular, empirical and rheological test results.

3.1. Correlations

A correlation analysis was performed using SPSS 15.0 commercial software. Spearman's correlation coefficient (ρ_{Spearman}) was used to discover whether there is any kind of association between two variables. This is a non-parametric correlation coefficient which is preferred to Pearson's correlation coefficient because it works regardless of the distributions of the variables and is less

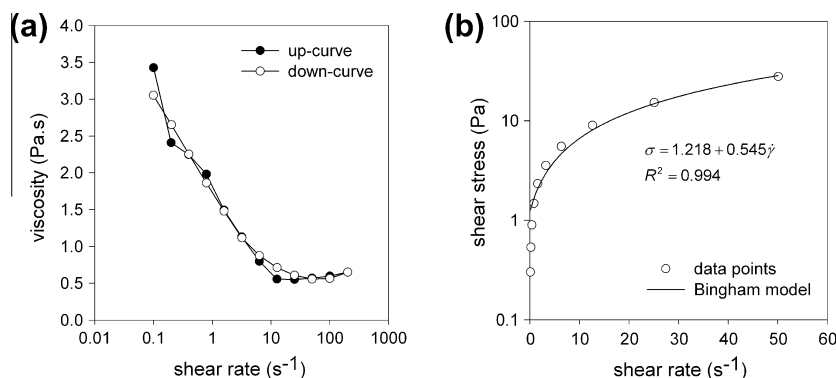


Fig. 3. (a) Up- and down-flow curves, and (b) fitted Bingham model to the down curve data.

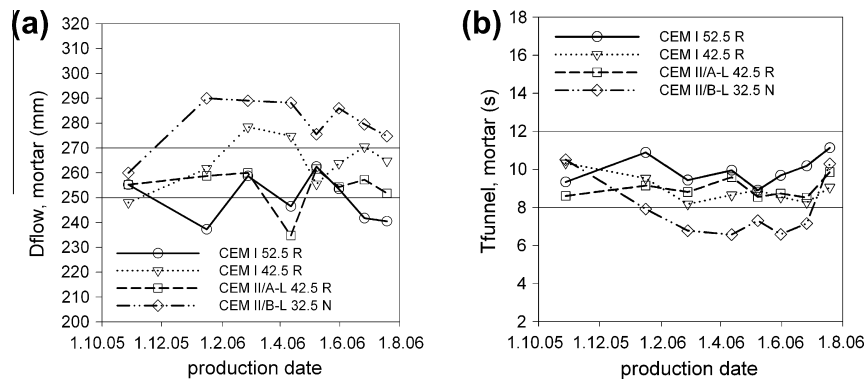


Fig. 4. Variation of (a) Dflow and (b) Tfunnel SCC-mortar results, with cement delivery.

Table 3

Properties of mortars and corresponding pastes incorporating CEM I 52.5 R from different deliveries.

Mix reference/ cement delivery	Mortar test results			Paste test results									
	Dflow (mm)	Tfunnel (s)	fc,28 (MPa)	Dflow (mm)	Tflow (s)	fc,28 (MPa)	w _{free} (kg/m ³)	σ ₀ (Pa)	η _{pl} (Pa s)	Temp. initial (°C)	Time acceler. (h)	Time peak (h)	Temp. peak (°C)
A/1st	255.25	9.35	67.64	–	–	–	–	–	–	–	–	–	–
A/2nd	237.25	10.89	72.42	143.50	43.65	80.27	66.58	1.218	0.545	22.8	6.4	12.3	37.1
A/3rd	258.75	9.44	71.49	159.50	36.73	88.14	71.56	0.577	0.357	23.0	6.6	12.7	37.5
A/4th	246.50	9.96	70.11	143.25	37.92	83.59	71.67	1.833	0.567	23.3	6.8	12.4	38.6
A/5th	262.50	8.91	68.68	160.00	36.58	88.44	72.50	0.643	0.410	23.3	6.5	12.4	36.8
A/6th	253.50	9.69	76.01	147.75	36.61	73.83	71.42	1.120	0.508	25.6	6.1	11.8	38.4
A/7th	241.75	10.19	59.08	145.75	35.17	73.88	70.42	1.297	0.564	27.2	5.9	11.0	38.7
A/8th	240.50	11.14	69.38	147.75	59.41	77.15	60.42	0.889	0.614	24.9	5.6	11.4	37.9
Mean	249.50	9.94	69.35	149.64	40.87	80.76	69.22	1.083	0.509	24.3	6.3	12.0	37.8
Std. dev.	9.29	0.77	4.89	7.13	8.63	6.19	4.34	0.431	0.093	1.6	0.4	0.6	0.8
B/1st	249.75	10.32	71.37	–	–	–	–	–	–	–	–	–	–
B/2nd	240.00	10.33	74.41	140.25	54.16	86.40	62.33	1.278	0.626	22.5	7.3	12.9	37.7
B/3rd	261.25	9.09	75.28	154.00	39.60	88.55	70.00	0.649	0.399	23.0	7.6	12.8	38.2
B/4th	251.50	9.38	73.62	140.00	44.42	88.55	68.83	2.185	0.639	23.3	7.0	12.5	39.3
B/5th	267.25	8.85	74.36	152.75	43.97	87.63	69.92	0.698	0.461	23.0	7.3	13.0	37.6
B/6th	259.50	8.97	69.97	142.75	42.67	80.32	68.50	1.227	0.568	25.1	6.8	12.2	38.3
B/7th	246.75	9.29	66.18	140.50	41.63	73.37	67.75	1.520	0.625	27.4	6.0	11.5	39.3
B/8th	251.50	10.02	75.83	143.50	67.88	82.36	59.08	1.000	0.679	24.9	6.1	11.6	39.2
Mean	253.44	9.53	72.63	144.82	47.76	83.88	66.63	1.222	0.571	24.2	6.9	12.4	38.5
Std. dev.	8.74	0.60	3.26	6.00	10.01	5.62	4.23	0.528	0.103	1.7	0.6	0.6	0.7
C/1st	251.25	10.02	73.40	–	–	–	–	–	–	–	–	–	–
C/2nd	246.00	10.33	85.52	136.25	66.07	86.20	57.67	1.486	0.694	22.5	7.3	12.8	38.1
C/3rd	272.75	8.13	80.68	152.50	48.72	93.09	64.00	0.685	0.424	23.0	7.6	13.0	37.7
C/4th	252.25	9.66	74.19	132.00	62.43	87.27	63.58	2.450	0.734	23.3	7.2	12.8	39.5
C/5th	266.00	8.98	73.34	148.00	54.09	88.70	63.92	0.851	0.511	23.0	7.3	13.4	37.4
C/6th	262.50	8.59	77.72	139.75	60.08	83.03	61.83	1.186	0.664	25.1	7.4	13.0	38.0
C/7th	246.50	9.50	75.50	133.00	72.70	80.01	58.83	1.376	0.761	27.4	6.7	12.3	39.3
C/8th	254.75	10.09	71.14	138.50	84.24	84.05	54.17	1.027	0.662	24.9	6.2	11.9	38.3
Mean	256.50	9.41	76.43	140.00	64.04	86.05	60.57	1.295	0.636	24.2	7.1	12.8	38.4
Std. dev.	9.63	0.78	4.70	7.63	11.82	4.24	3.79	0.582	0.123	1.7	0.5	0.5	0.8

affected by outliers [21]. High absolute values of a correlation coefficient (that is values close to 1) only indicate that variables are associated with each other, not that one variable causes another. There are also negative relations but the important quality of these correlation coefficients in the present study is not their sign but their absolute value.

3.2. Workability variations

Effect of cement delivery on SCC mortar fresh properties is presented in Fig. 4, along with the established acceptance limits. This figure includes only results of mortar mixes with constant $V_s/V_m = 0.5$ and $w/c = 0.45$. Coefficients of variation associated to the mixing process and testing procedure themselves were of about

1% and 2.5% for Dflow and Tfunnel results, respectively. In general, a random variation of results was observed between deliveries (Fig. 4), falling within or not exceeding by far the target ranges (Dflow = 260 ± 10 mm and Tfunnel = 10 ± 2 s), except in the case of CEM II/B-L 32.5 N. Since the mix proportions were optimized for the first delivery and maintained constant, in spite of the relatively small variation of results, beyond the second delivery all the CEM II/B-32.5 N mortar results fell outside the target ranges. This simple example illustrates the importance of an efficient quality control to detect large deviations from the targets and hence implement corrective actions in order to maintain the results in conformity with the performance requirements. From our experience, a standard deviation of mortar Dflow of the order of those shown in Tables 3–6 (from 8.5 to 11.5) is recommended for quality

Table 4

Properties of mortars and corresponding pastes incorporating CEM I 42.5 R from different deliveries.

Mix reference/ cement delivery	Mortar test results			Paste test results									
	Dflow (mm)	Tfunnel (s)	$f_{c,28}$ (MPa)	Dflow (mm)	Tflow (s)	$f_{c,28}$ (MPa)	w_{free} (kg/m ³)	σ_0 (Pa)	η_{pl} (Pa s)	Temp. initial (°C)	Time acceler. (h)	Time peak (h)	Temp. peak (°C)
A/1st	248.00	10.33	64.41	–	–	–	–	–	–	–	–	–	–
A/2nd	261.75	9.54	63.55	164.25	19.93	71.89	81.00	0.478	0.334	21.5	7.4	14.7	31.7
A/3rd	278.50	8.19	58.84	181.75	19.14	70.41	81.58	0.310	0.333	23.1	7.4	14.2	33.0
A/4th	274.75	8.66	56.68	166.50	22.11	65.20	81.08	0.567	0.360	23.1	6.5	13.2	33.4
A/5th	255.50	8.91	59.52	162.50	20.80	65.81	82.25	0.653	0.386	25.6	7.1	13.3	33.7
A/6th	263.75	8.55	56.77	163.25	21.66	71.58	82.50	0.598	0.383	22.7	6.8	13.2	33.8
A/7th	270.50	8.27	54.21	168.50	18.39	59.47	83.42	0.293	0.329	26.7	6.7	12.9	34.3
A/8th	264.75	9.06	51.13	169.75	21.70	63.05	80.67	0.510	0.344	24.5	6.7	13.3	33.0
Mean	264.69	8.94	58.14	168.07	20.53	66.77	81.79	0.487	0.353	23.9	6.9	13.5	33.3
Std. dev.	9.99	0.71	4.47	6.60	1.42	4.71	0.98	0.139	0.024	1.8	0.4	0.6	0.8
B/1st	258.25	9.60	72.48	–	–	–	–	–	–	–	–	–	–
B/2nd	265.25	9.66	68.60	150.25	40.44	79.60	69.67	0.895	0.553	21.5	8.8	16.3	33.3
B/3rd	284.50	7.52	69.62	157.00	34.49	78.53	71.92	0.691	0.526	23.1	9.2	15.4	34.9
B/4th	273.00	8.13	71.46	150.50	38.08	71.63	69.67	0.928	0.545	22.9	8.0	13.8	35.1
B/5th	264.50	8.10	64.74	145.00	39.13	73.73	70.50	1.034	0.603	25.1	8.4	14.4	34.9
B/6th	275.00	7.81	63.31	150.00	40.43	73.22	70.50	0.877	0.586	23.1	7.8	14.4	35.6
B/7th	281.88	6.88	59.20	154.75	33.75	65.04	73.83	0.545	0.509	26.3	8.2	14.4	35.5
B/8th	279.75	7.56	62.53	144.50	36.01	69.90	70.75	0.978	0.548	24.2	7.3	14.2	34.6
Mean	272.77	8.15	66.49	150.29	37.47	73.09	70.98	0.850	0.553	23.7	8.2	14.7	34.8
Std. dev.	9.34	0.99	4.73	4.59	2.76	4.99	1.47	0.172	0.032	1.6	0.6	0.8	0.8
C/1st	254.25	10.11	74.10	–	–	–	–	–	–	–	–	–	–
C/2nd	266.75	9.08	70.95	142.50	48.13	81.19	66.11	1.168	0.592	21.5	8.8	16.3	33.3
C/3rd	293.50	7.31	70.36	154.25	40.52	81.03	67.89	0.718	0.560	23.1	9.2	15.7	34.7
C/4th	273.00	8.33	70.03	146.25	51.77	77.87	66.11	1.055	0.619	22.8	8.0	14.2	36.2
C/5th	265.75	7.43	67.03	134.25	56.99	77.71	64.42	1.222	0.624	25.1	8.4	14.6	36.5
C/6th	277.50	7.66	64.06	147.00	50.30	83.54	66.11	0.958	0.642	24.2	8.1	15.0	35.6
C/7th	278.50	7.30	61.30	153.25	42.78	67.04	69.44	0.589	0.561	26.3	8.4	14.9	35.9
C/8th	270.00	8.02	67.24	139.00	56.40	72.91	66.11	1.023	0.612	23.9	7.8	14.8	34.1
Mean	272.41	8.15	68.13	145.21	49.55	77.33	66.60	0.962	0.601	23.8	8.4	15.1	35.2
Std. dev.	11.46	1.00	4.10	7.26	6.29	5.67	1.61	0.231	0.032	1.6	0.5	0.7	1.2

Table 5

Properties of mortars and corresponding pastes incorporating CEM II/A-L 42.5 R from different deliveries.

Mix reference/ cement delivery	Mortar test results			Paste test results									
	Dflow (mm)	Tfunnel (s)	$f_{c,28}$ (MPa)	Dflow (mm)	Tflow (s)	$f_{c,28}$ (MPa)	w_{free} (kg/m ³)	σ_0 (Pa)	η_{pl} (Pa s)	Temp. initial (°C)	Time acceler. (h)	Time peak (h)	Temp. peak (°C)
A/1st	255.25	8.61	60.50	–	–	–	–	–	–	–	–	–	–
A/2nd	258.75	9.16	59.74	159.25	22.82	73.78	81.50	0.532	0.269	21.3	6.4	13.0	32.8
A/3rd	260.00	8.82	61.01	158.00	24.33	63.00	77.33	0.703	0.352	22.2	6.4	14.0	30.7
A/4th	234.75	9.60	59.06	148.50	24.94	61.98	75.25	0.728	0.224	23.6	5.3	11.2	33.5
A/5th	261.50	8.56	56.97	165.50	24.35	69.33	79.50	0.516	0.281	23.7	5.9	12.8	32.8
A/6th	254.25	8.74	51.48	157.50	21.99	61.57	81.75	0.873	0.409	25.6	5.8	13.4	31.6
A/7th	257.25	8.52	58.32	156.75	21.66	63.31	80.42	0.982	0.413	25.1	5.4	12.0	33.9
A/8th	251.75	9.86	61.11	153.75	32.72	63.61	71.75	1.133	0.497	25.2	5.0	11.5	33.8
Mean	254.19	8.98	58.52	157.04	24.68	65.22	78.21	0.781	0.349	23.8	5.7	12.6	32.7
Std. dev.	8.47	0.51	3.17	5.19	3.76	4.57	3.68	0.229	0.097	1.6	0.5	1.0	1.2
B/1st	258.50	8.57	65.15	–	–	–	–	–	–	–	–	–	–
B/2nd	264.50	7.82	69.64	148.50	34.71	83.03	71.67	0.846	0.458	21.9	7.6	14.2	35.2
B/3rd	268.75	7.39	67.79	147.50	39.41	77.30	69.25	1.246	0.545	22.0	7.6	15.0	32.6
B/4th	244.25	8.40	60.91	138.25	46.01	73.01	68.17	0.737	0.401	23.3	7.1	12.8	35.4
B/5th	275.00	7.88	70.09	151.00	40.05	79.04	71.08	0.703	0.451	23.5	6.9	13.9	36.0
B/6th	260.50	7.22	65.92	142.25	43.11	73.68	69.75	1.057	0.583	25.4	7.4	15.1	33.2
B/7th	266.75	7.33	64.13	141.00	44.91	75.41	69.58	1.293	0.613	24.9	6.6	13.4	36.7
B/8th	261.75	7.99	65.48	140.25	62.50	73.73	62.17	1.125	0.685	25.2	6.3	13.2	35.9
Mean	262.50	7.82	66.14	144.11	44.38	76.46	68.81	1.001	0.534	23.7	7.1	13.9	35.0
Std. dev.	9.03	0.49	3.01	4.84	8.85	3.62	3.15	0.240	0.101	1.5	0.5	0.9	1.5
C/1st	256.00	8.59	69.12	–	–	–	–	–	–	–	–	–	–
C/2nd	266.50	7.91	71.18	134.50	62.89	87.88	63.33	1.315	0.606	22.1	7.6	14.5	36.2
C/3rd	260.50	7.63	70.92	128.50	64.50	82.87	64.75	1.813	0.672	22.4	7.7	15.0	34.7
C/4th	238.00	8.31	71.42	127.00	76.16	78.68	59.25	1.142	0.505	23.5	7.1	13.0	37.1
C/5th	272.25	7.10	76.41	137.00	67.66	85.38	62.92	0.982	0.568	23.5	7.4	14.6	36.5
C/6th	258.75	7.09	65.88	133.50	64.66	78.38	62.67	1.437	0.697	25.4	7.6	15.2	34.8
C/7th	256.50	7.31	64.83	140.00	77.58	81.03	61.50	1.229	0.652	24.8	7.0	14.0	37.1
C/8th	250.75	8.27	71.20	125.25	96.46	82.62	55.17	1.905	0.780	25.2	6.1	12.7	37.0
Mean	257.41	7.77	70.12	132.25	72.84	82.41	61.37	1.403	0.640	23.8	7.2	14.1	36.2
Std. Dev.	10.27	0.58	3.61	5.48	11.93	3.44	3.22	0.343	0.090	1.3	0.6	1.0	1.0

Table 6

Properties of mortars and corresponding pastes incorporating CEM II/B-L 32.5 N from different deliveries.

Mix reference/ cement delivery	Mortar test results			Paste test results									
	Dflow (mm)	Tfunnel (s)	fc,28 (MPa)	Dflow (mm)	Tflow (s)	fc,28 (MPa)	w _{free} (kg/ m ³)	σ ₀ (Pa)	η _{pl} (Pa s)	Temp. initial (°C)	Time acceler. (h)	Time peak (h)	Temp. peak (°C)
A/1st	260.00	10.52	49.78	–	–	–	–	–	–	–	–	–	–
A/2nd	290.00	7.92	45.71	184.00	19.04	49.61	85.58	0.157	0.225	21.9	5.9	13.8	23.9
A/3rd	289.00	6.78	46.98	177.25	14.85	47.11	90.75	0.243	0.179	22.9	4.9	14.0	26.0
A/4th	288.25	6.58	45.90	180.00	16.16	46.80	88.67	0.492	0.284	23.1	5.3	15.9	27.0
A/5th	275.50	7.31	44.55	168.75	15.35	47.93	89.33	0.383	0.209	24.5	5.3	15.7	26.5
A/6th	286.00	6.59	43.12	178.25	16.42	44.81	88.50	0.352	0.261	24.4	5.0	11.1	26.1
A/7th	279.50	7.16	41.84	160.75	17.29	45.32	86.67	0.359	0.311	26.7	4.8	10.8	26.3
A/8th	274.75	10.30	37.09	174.50	20.38	44.25	84.08	0.307	0.320	24.5	4.9	11.7	26.5
Mean	280.38	7.89	44.37	174.79	17.07	46.55	87.65	0.327	0.255	24.0	5.2	13.3	26.0
Std. dev.	10.23	1.61	3.80	7.79	2.00	1.89	2.32	0.107	0.053	1.5	0.4	2.1	1.0
B/1st	262.75	8.69	58.14	–	–	–	–	–	–	–	–	–	–
B/2nd	292.00	6.75	53.56	171.50	24.38	56.41	79.08	0.235	0.265	21.4	5.9	13.7	24.7
B/3rd	290.25	5.30	53.87	171.25	18.29	56.61	85.50	0.301	0.207	22.6	5.1	14.6	26.3
B/4th	294.00	5.61	53.76	166.75	20.47	54.11	82.83	0.669	0.352	22.9	5.2	15.4	27.7
B/5th	287.00	5.63	50.98	161.75	19.79	51.60	82.17	0.515	0.252	24.5	5.4	15.2	27.1
B/6th	292.00	5.51	51.34	165.25	19.19	53.50	82.67	0.508	0.283	24.0	5.0	11.3	26.4
B/7th	286.50	5.74	48.09	156.75	23.91	50.58	79.75	0.535	0.369	26.2	5.1	10.9	26.5
B/8th	299.00	5.77	45.92	165.75	27.22	50.94	78.83	0.433	0.377	23.6	4.8	11.7	26.6
Mean	287.94	6.12	51.96	165.57	21.89	53.39	81.55	0.457	0.301	165.57	21.89	53.39	81.55
Std. dev.	10.92	1.12	3.79	5.19	3.30	2.49	2.44	0.148	0.066	1.5	0.4	1.9	0.9
C/1st	257.75	8.41	67.17	–	–	–	–	–	–	–	–	–	–
C/2nd	289.25	6.13	62.52	163.25	31.10	65.71	73.33	0.354	0.339	21.3	5.2	12.9	25.3
C/3rd	281.75	5.32	57.96	154.00	23.81	65.76	78.25	0.593	0.259	22.9	5.0	13.8	27.8
C/4th	284.00	5.24	56.92	150.00	26.46	61.98	77.00	0.938	0.421	22.9	5.0	14.4	28.9
C/5th	272.50	5.25	60.68	148.00	25.09	62.44	76.83	0.826	0.300	24.5	5.0	14.0	28.5
C/6th	277.00	5.25	60.34	148.50	28.91	60.85	75.33	0.755	0.372	24.0	4.9	11.0	27.7
C/7th	275.25	5.28	55.28	144.00	32.39	58.91	72.75	0.767	0.440	26.2	4.7	10.6	27.4
C/8th	293.25	5.13	50.69	145.50	33.91	58.91	72.67	0.643	0.443	23.5	4.7	11.2	27.7
Mean	278.84	5.75	58.95	150.46	28.81	62.08	75.17	0.697	0.368	23.6	4.9	12.6	27.6
Std. dev.	11.03	1.12	4.96	6.49	3.84	2.84	2.28	0.189	0.072	1.5	0.2	1.6	1.2

Table 7Correlation matrix within cement characteristics and between cement characteristics and SCC mortar/paste test results, corresponding to CEM II/B-L 32.5 N. Results with very strong correlation (>0.85) are underlined and typed bold, and with the strong correlation (0.75–0.85) are typed **bold**.

	LOI	SA (Blaine)	Residue 45 μm	(Na ₂ O)eq.	SO ₃	Free CaO	C ₃ S	C ₂ S	C ₃ A
LOI	1.000								
SA (Blaine)	–0.571	1.000							
Residue 45 μm	0.084	0.180	1.000						
(Na ₂ O)eq.	–0.214	0.357	0.060	1.000					
SO ₃	–0.690	0.524	–0.347	0.357	1.000				
Free CaO	–0.301	0.590	0.758*	0.048	0.133	1.000			
C ₃ S	–0.321	0.143	0.018	–0.107	–0.429	–0.164	1.000		
C ₂ S	0.214	–0.214	0.072	0.000	0.286	0.109	–0.714	1.000	
C ₃ A	–0.143	0.071	0.000	0.143	0.179	0.436	–0.357	–0.179	1.000
Dflow ^a	0.357	–0.881**	–0.287	–0.405	–0.524	–0.590	0.179	–0.321	0.179
Tfunnel ^a	–0.619	0.524	–0.252	0.738*	0.857**	0.012	–0.250	0.286	–0.036
fc,28 ^a	–0.071	–0.190	0.611	0.405	–0.333	0.157	0.357	–0.250	–0.071
Dflow ^b	0.214	–0.714	0.180	0.071	–0.143	0.000	–0.393	0.036	0.643
Tflow ^b	–0.643	0.429	–0.649	0.071	0.893**	0.109	–0.429	0.107	0.571
fc,28 ^b	0.286	–0.500	–0.216	0.571	–0.286	–0.764*	0.286	–0.429	–0.107
w _{free} ^b	0.643	–0.429	0.649	–0.071	–0.893**	–0.109	0.429	–0.107	–0.571
σ ₀ ^b	0.393	0.536	0.577	–0.036	–0.536	0.600	0.250	–0.393	0.107
η _{pl} ^b	–0.571	0.750	–0.162	–0.214	0.500	0.655	–0.143	–0.036	0.536
Temp. initial ^b	–0.107	0.893**	–0.072	–0.107	0.179	0.273	0.179	–0.107	–0.321
Time acceler. ^b	0.536	–0.536	0.126	0.500	–0.286	–0.218	–0.286	–0.179	0.500
Time peak ^b	0.571	–0.357	0.432	0.571	–0.679	0.000	0.143	–0.107	0.143
Temp. peak ^b	0.286	0.607	0.450	0.214	–0.357	0.655	0.107	–0.143	0.214

* Significant at the 0.05 level (two-tailed).

** Significant at the 0.01 level (two-tailed).

^a Mortar test results.^b Paste test results.

control of SCC. It should be noted that the observed variations of SCC fresh mortar properties could not be anticipated from results of the standard water demand test since this test does not take into

account the effect of the superplasticizer. The problem with workability variations is that they can result in a larger range of variation of the hardened state properties, due to the occurrence of

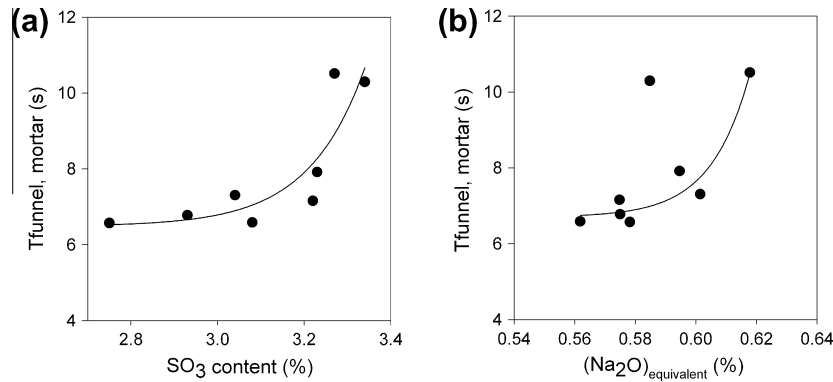


Fig. 5. Effects of (a) SO_3 and (b) $(\text{Na}_2\text{O})_{\text{equivalent}}$ on T_{funnel} of mortars incorporating CEM II/B-L 32.5 N.

Table 8

Correlation matrix within all SCC paste test results. Results with very strong correlation (>0.85) are underlined and typed **bold**, and with strong correlation (0.75 – 0.85) are typed **bold**.

	Dflow	Tflow	$f_{c,28}$	w_{free}	σ_0	η_{pl}	Temp. initial	Time acceler.	Time peak	Temp. peak
Dflow	1.000	<u>−0.889</u> **	−0.641**	<u>0.881</u> **	<u>−0.902</u> **	<u>−0.853</u> **	−0.192	−0.386**	0.037	−0.678**
Tflow		1.000	<u>0.797</u> **	<u>−0.986</u> **	<u>0.791</u> **	<u>0.894</u> **	0.074	0.533**	0.030	<u>0.769</u> **
$f_{c,28}$			1.000	<u>−0.794</u> **	0.646**	0.697**	−0.184	0.643**	0.066	<u>0.836</u> **
w_{free}				1.000	<u>−0.797</u> **	<u>−0.890</u> **	−0.074	−0.529**	−0.008	<u>−0.780</u> **
σ_0					1.000	<u>0.869</u> **	0.174	0.379**	−0.018	0.714**
η_{pl}						1.000	0.228*	0.548**	0.057	<u>0.754</u> **
Temp. initial							1.000	−0.198	−0.353**	0.201
Time acceler.								1.000	0.570**	0.484**
Time peak									1.000	−0.180
Temp. peak										1.000

* Significant at the 0.05 level (two-tailed).

** Significant at the 0.01 level (two-tailed).

segregation or lack of filling ability. This explains the variation of compressive strength results of SCC mortars (the coefficients of variation varied from 5.4% to 8.6%). Again, these results could not be anticipated from standard compressive strength results (without superplasticizer), which exhibited coefficients of variation varying from 2.4% to 3.8%.

The initial reactivity of cement is critical for the performance of a polycarboxylate type superplasticizer. Higher dosages of superplasticizer are required with an increase of cement fineness, an increase of C_3A phase at the surface of cement particles or an increase of quickly soluble sulfates ions (especially, from alkali sulfate) [22]. Considering CEM II/B-L 32.5 N mixture results, which exhibited the largest deviation from the targets, a correlation matrix within cement characteristics and between cement characteristics and SCC mortar/paste test results is presented in Table 7. Selected explanatory variables were: loss on ignition; surface area (Blaine); residue in the 45 μm sieve; $(\text{Na}_2\text{O})_{\text{equivalent}}$ content; SO_3 content; free CaO; C_3S , C_2S and C_3A contents of cement. High correlations between explanatory variables increase the difficulty of associating certain mortar/paste properties to cement properties because it is not clear how much of an effect should be attributed to each mortar/paste property. In the case of CEM II/B-L 32.5 N only a significant correlation was found between (free CaO) and (residue 45 μm). The SO_3 content of CEM II/B-L 32.5 N was the most relevant effect to explain the observed variations in mortar T_{funnel} , paste T_{flow} and paste w_{free} (see Table 7). A significant correlation was also found between mortar T_{funnel} and $(\text{Na}_2\text{O})_{\text{equivalent}}$ content of cement. The effect of surface area (Blaine) was significant to explain the variations of mortar Dflow and the temperature of paste in the beginning of the semi-adiabatic calorimeter test. Based on the experience of the cement producer, the specific surface area

obtained by the Blaine method is not a good indicator of Type II cement fineness. In this case, the 50% percentile ($D_{0.5}$) of the particle size distribution is a better indicator of cement fineness, but no significant correlation was found between ($D_{0.5}$) and (Dflow, mortar) nor between ($D_{0.5}$) and (Temp initial), for CEM II/B-L 32.5 N results ($\rho_{\text{Spearman}} = 0.048$ and $\rho_{\text{Spearman}} = -0.286$, respectively). Thus, only the effects of SO_3 and $(\text{Na}_2\text{O})_{\text{equivalent}}$ contents were considered the most relevant for the observed variations, in the fresh state (see Fig. 5). It can be observed that mortar T_{funnel} increased with an increase of SO_3 and $(\text{Na}_2\text{O})_{\text{equivalent}}$ contents in cement.

Various authors referenced by [22] found that the fluidity of cement paste prepared using the polycarboxylate type superplasticizer depends upon the content of alkali sulfate. One of the suggested explanations is that the side chains of PC polymer are shrunk by using mixing water containing high concentration of ions, thereby decreasing the dispersing action of a polycarboxylate type superplasticizer. But Hanehara and Yamada [22] found that lowering of the fluidity of cement paste by adding alkali sulfate is attributed to the reduction of the amount of the admixture adsorbed on cement caused by adding the sulfate ions. Thus, a possible explanation for the fluidity variations observed with CEM II/B-L 32.5 N mortars is a variation of alkali sulfate content in cement, which can be expected from the results of SO_3 and $(\text{Na}_2\text{O})_{\text{equivalent}}$ contents in cement (see Fig. 5). An increase of alkali sulfate content reduces the dispersing action of the superplasticizer, lowering the amount of free water and, consequently, reducing the fluidity which is indicated by higher flow time results. Sulfates are supplied by both alkali sulfates and calcium sulfates. The type of calcium sulfate also matters, as dehydrated forms supply sulfate ions faster than gypsum. A high correlation was not found between the SO_3 cement content and spread flow of mortar or paste because

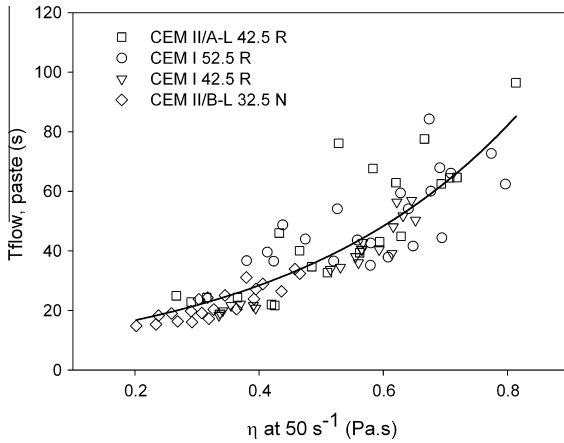


Fig. 6. Relation between the viscosity at a shear rate of 50 s^{-1} and flow time of pastes ($\rho_{\text{Spearman}} = 0.902$).

the family of the orifice tests, like Marsh cone and V-funnel tests, are more sensitive to variations in paste free water content, and therefore are often used for quality control of grouts.

3.3. Empirical vs. rheology paste test results

In order to verify if the different test results obtained on pastes correlate with each other, a correlation matrix within paste test results was computed, including results obtained for all cement types and cement deliveries (see Table 8).

3.3.1. Flow time

In Fig. 6 flow time results of pastes in the Marsh cone are plotted against the measured viscosity at 50 s^{-1} of shear rate, from the down-curve, measured at 35 min after the beginning of mixing. The corresponding ρ_{Spearman} was 0.902 (significant at the 0.01 level (two-tailed)) indicating that results of both tests are clearly related. However one notices that the scatter of both flow time and viscosity increased at increasing flow time. This was also found by other authors [15,23,24]. The correlation coefficient between flow time and viscosity decreased for lower shear rates. For example, the correlation coefficient between flow time and the viscosities measured at 12.6 s^{-1} and 1.6 s^{-1} was 0.858 and 0.853, respectively. At higher shear rates, the particles are ‘fully’ dispersed and thus the results are less affected by time effects and shear history, which might explain the lower dispersion of results and the higher correlation coefficients. A similar correlation coefficient was also found between flow time and plastic viscosity (Bingham model), as shown in Table 8. The viscosity is almost equal to the plastic viscosity at high shear rates. However, at lower shear rates the viscosity is much higher than the plastic viscosity.

According to Roussel and Le Roy [16] flow time, measured with the Marsh cone, is proportional to viscosity but yield stress has to be taken into account to predict flow time of non-Newtonian fluids, like the case of cement pastes. The presence of yield stress increases the time needed for a certain amount to flow out of the cone [16]. The following relation between flow time and rheological parameters of paste was validated for different cone geometries and various SCC cement pastes by Roussel and Le Roy [16]:

$$T_{\text{flow}} = \frac{a_v \eta_{pl}}{\rho - b_v \sigma_0} \quad (3)$$

where a_v and b_v are constants, depending on cone geometry and the observed flowing volume V , ρ is the material density, and η_{pl} and σ_0 are the plastic viscosity and yield stress, respectively. The constants

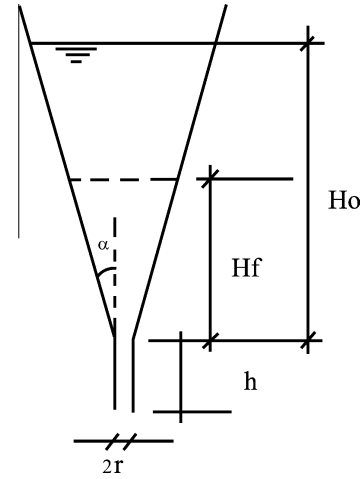


Fig. 7. α , r , H_0 and h dependent on cone geometry and filling volume [16].

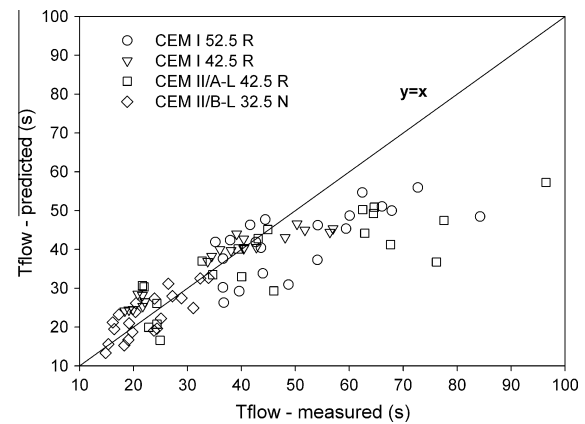


Fig. 8. Comparison between measured and predicted flow time.

a_v and b_v can either be calibrated using known materials or calculated using the following expressions:

$$a_v = \frac{8V \tan(\alpha) [3h(H_0 \tan(\alpha) + r)^3 + H_0 r (H_0^2 \tan^2(\alpha) + 3H_0 r \tan(\alpha) + 3r^2)]}{[3\pi r^3 \tan(\alpha) g r (h + H_0)] (H_0 \tan(\alpha) + r)^3} \quad (4)$$

$$b_v = \frac{\pi r^3 [8r \ln(H_0 \tan(\alpha) + r) - 8r \ln(r) + 8h \tan(\alpha)]}{3\pi r^3 \tan(\alpha) g r (h + H_0)} \quad (5)$$

where α , r , H_0 and h can be obtained from the cone geometry and filling volume V , as indicated in Fig. 7, and g is the gravitational constant [16]. a_v and b_v are very sensitive to r and h , which sometimes are difficult to measure, therefore estimation of these constants is sometimes preferred [16]. A comparison between measured flow time and predicted flow time using Eq. (3) is given in Fig. 8, with $a_v = 154,503 \text{ s}^2/\text{m}^2$ and $b_v = 25.5 \text{ s}^2/\text{m}^2$. From this figure it can be observed that up to a flow time of approximately 50 s the model given by Eq. (3) adequately predicts the measured flow times. For flow times above 50 s, Roussel and Le Roy's model underestimate Tflow. This may be due to differences in testing techniques used to determine yield stress.

The variability of the flow time results and loss of fluidity with time increases with increasing paste viscosity, which is a major disadvantage of the Marsh flow test. This was also found by Gomes [15] and Le Roy and Roussel [24]. In this study, a strong relation was found between flow time (Marsh cone) and free water

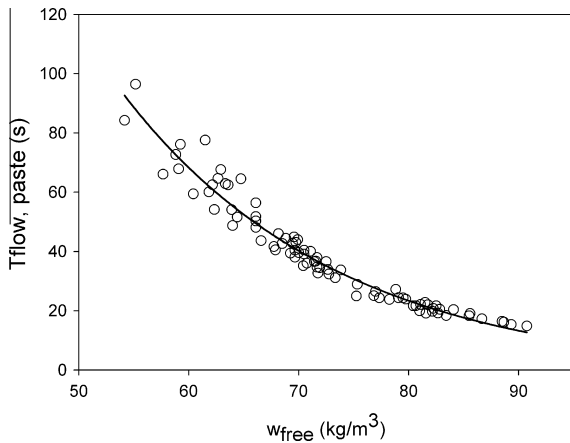


Fig. 9. Relation between w_{free} and T_{flow} of SCC pastes ($\rho_{\text{spearman}} = -0.986$).

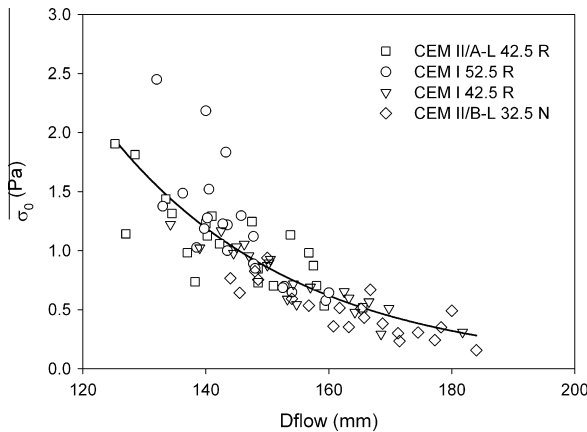


Fig. 10. Relation between the yield stress and flow diameter of pastes ($\rho_{\text{spearman}} = -0.902$).

(centrifuge test) results (see Fig. 9 and Table 8). Therefore, the centrifuge test is a promising substitute test of the Marsh cone with the advantage of being equally precise for lower and higher fluidity pastes. Unfortunately, application of classical regression methods failed to establish a statistical model relating flow time to free water that guarantees quality of predictions, due to heteroscedasticity of residuals, requiring further research.

3.3.2. Spread flow diameter

Several authors reported a relation between yield stress and slump, as well as spread flow (of concrete, mortars or paste) [25–28]. However, different relations can be found in the literature. A comparison between two models relating yield stress with spread radius and its range of validity is presented in [25]. Saak's model (first developed by Murata) [27] is given by

$$\sigma_0 = \frac{\rho V g}{\sqrt{3\pi R^2}} \quad (6)$$

where ρ and V are the density and volume of the sample (assuming that the cone is completely filled up), respectively, and R is the radius of the spread. Flatt et al. [25] clarified that this model performs well at low spread radius and not at large spread radius. In contrast, Roussel's model, developed within the framework of the long-wave approximation, given by

$$\sigma_0 = 1.747 \rho V^2 R^{-5} - \lambda \frac{R^2}{V} \quad (7)$$

where λ is a constant [28], was found to be more reliable for large spreads (sample height must be small compared to the sample spread for the long-wave approximations to be relevant) [25]. Generally λ is a function of both the unknown tested fluid surface tension and contact angle. A value of 0.005 was adopted by Roussel et al. [28] for similar experiments. In addition, an exponential function of the type of

$$\sigma_0 = a \exp(-bR) \quad (8)$$

where a and b are fitting parameters, was found to approximately fit experimental data over a wide range of diameters of interest [25]. The data collected in the present work supports this conclusion, as illustrated in Fig. 10. In this figure mini-slump flow diameter results of pastes are plotted against the yield stress (Bingham model), for measurements carried out 35 min after beginning of the mixing. The corresponding ρ_{spearman} was 0.902 (see Table 8).

The predictions of both the Saak and the Roussel models (Eqs. (6) and (7) with $\lambda = 0, 0.005$) are given in Fig. 11, for the range of spread diameters that can be obtained with Kantro's mini-slump cone. As can be observed in this figure, the yield stress data collected in the present work is closer to the curve described by Roussel's model with surface tension effects included. Nevertheless, this model failed to explain the relation between the spread diameter and yield stress results obtained in the current study. The divergence of data from Roussel's model can also be attributed to differences in how yield stress is determined.

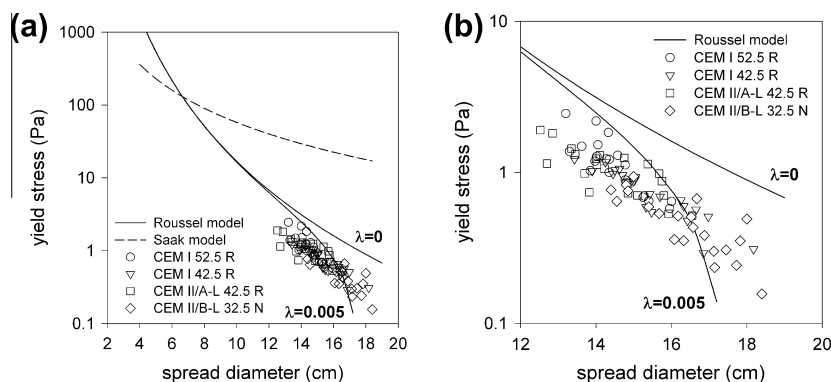


Fig. 11. Relation between yield stress and spread diameter calculated with Saak's model and Roussel's model (with both $\lambda = 0$ and 0.005) for the mini-slump cone (Kantro) and experimental data collected in the present study.

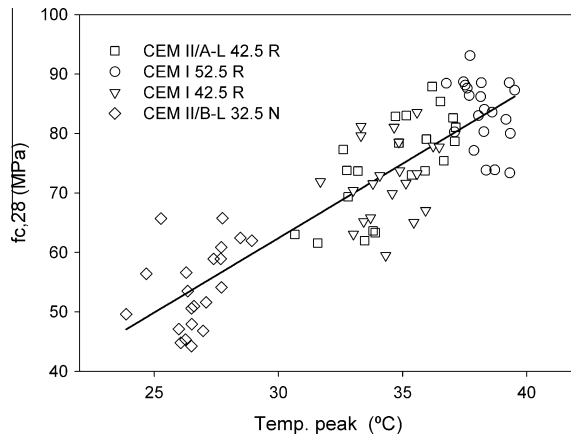


Fig. 12. Relation between the peak temperature and compressive strength (28 days) of pastes ($\rho_{\text{spearman}} = 0.836$).

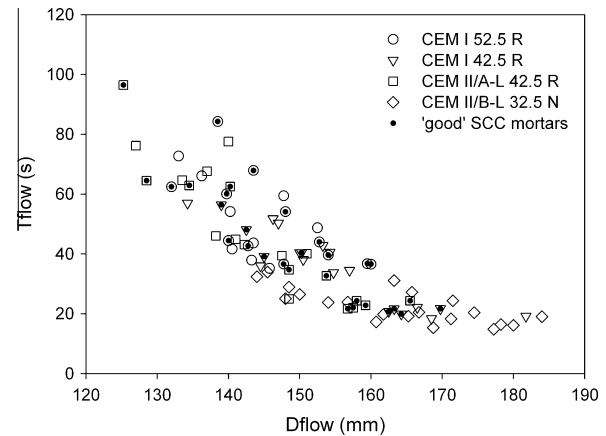


Fig. 13. Range of properties of the analysed pastes incorporating different cement types ($\rho_{\text{spearman}} = -0.889$).

3.3.3. Compressive strength

It is also noteworthy the relation found between 28 day paste compressive strength and the maximum temperature results obtained in the semi-adiabatic calorimeter test ($\rho_{\text{spearman}} = 0.986$; see Fig. 12 and Table 8). This relation can be very valuable because it allows estimating paste compressive strength at 28 days from results collected within the first hours of paste curing (less than 48 h). Considering only the cement characteristics, the peak temperature measured in the semi-adiabatic calorimeter test is mainly controlled by the intense hydration of C_3S , associated with the formation of C–S–H phases and the precipitation of portlandite, and cement fineness. On the other hand, C_3S , C_2S and cement fineness are the most influencing factors on late strength of mortars (28 days). Therefore, a strong correlation between T_{max} and $f_{c,28}$ results of mortars could be expected. In Fig. 12 one can clearly distinguish CEM I 52.5 R (highest C_3S content and lowest 45 μm residue) results from CEM II B-L 32.5 N (lowest C_3S content and highest 45 μm residue) results. The two other cements were similar in terms of chemical composition and fineness.

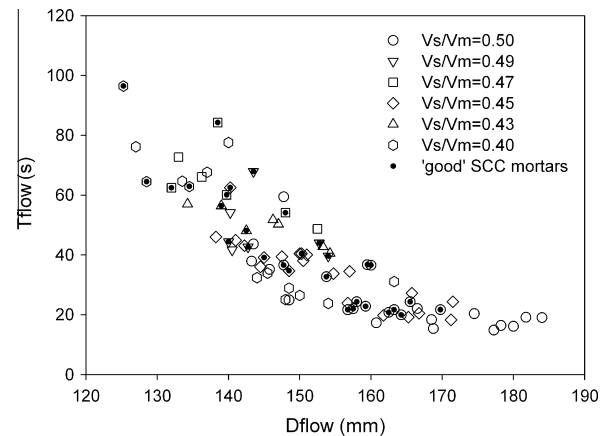


Fig. 14. Range of properties of the analysed pastes, corresponding to different V_s/V_m .

3.4. SCC paste target areas

The complete experimental programme included mortar mixtures with V_s/V_m ranging from 40% to 50%, w/c ratio ranging from 0.33 to 0.45, Sp/p ranging from 1.4% to 2%, and four different cement types. In addition, changes in mortar/paste properties were introduced due to variations in cement, from different deliveries. Altogether, it resulted in a large range of paste properties, which correspond to 'good' or 'near-good' SCC mortars, as can be observed in Fig. 13. The paste properties which led to mortar mixtures with $D_{\text{flow}} = 260 \pm 10$ mm and $T_{\text{funnel}} = 10 \pm 2$ s, considered here as 'good' SCC mortars, are identified with a black dot. These are spread over the entire area except in the lower part on the right, for D_{flow} values higher than about 170 mm. Thus, one can conclude that there is a target area of paste properties which can lead to 'good' SCC mortars (exhibiting $D_{\text{flow}} = 260 \pm 10$ mm and $T_{\text{funnel}} = 10 \pm 2$ s, simultaneously). In Fig. 14, data points are distinguished in terms of fine aggregate content (V_s/V_m) instead of cement type. From this figure it can be clearly seen that target paste properties are related to aggregate content. Mortars with higher fine aggregate content (V_s/V_m) require more fluid pastes to be flowable, while mortars with lower fine aggregate content require more viscous pastes to be stable.

Based on the target area defined in Fig. 14 and on the mini-slump flow and Marsh flow tests the mixtures can be optimized first on the paste level to minimize the number of tests on the mor-

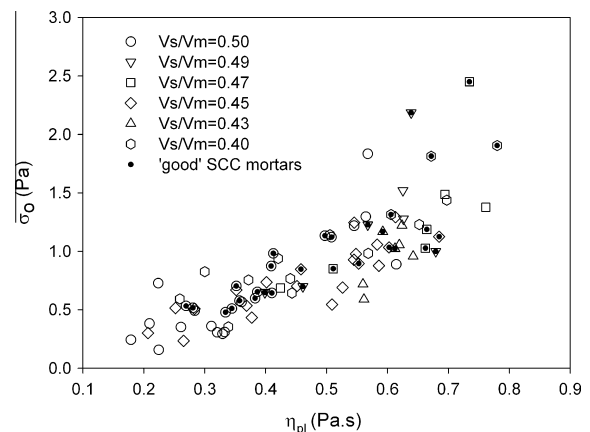


Fig. 15. Range of rheological parameters of the analysed pastes.

tar/concrete levels. However, tests on concrete must be carried out to verify the final paste composition and define the aggregates phase. In Fig. 15, the range of rheological parameters values (Bingham model) obtained in this study are presented along with the identification of those which led to 'good' SCC mortars. 'Good' SCC mortars were found for pastes with a plastic viscosity ranging

from about 0.3 to 0.8 Pa s and a yield stress ranging from 0.5 to 2.5 Pa. It should be mentioned that the target areas defined in Figs. 14 and 15 will probably change if a different superplasticizer or a viscosity agent (admixture or a very fine material) is used [23,29].

4. Conclusions

Based on presented results, the following conclusions can be drawn:

1. Large deviations from target workability properties can occur depending only on cement delivery, as occurred for CEM II/B-L 32.5 N. Thus, cement variations and cement-superplasticizer interaction should be taken into account when discussing robustness of SCC mixtures.
2. This study highlighted the importance of an efficient quality control of cement to detect large deviations from target and hence implement corrective actions in order to maintain cement paste fluidity results in conformity with performance requirements. However, standard tests on cement like setting time and water demand are not adequate because they do not incorporate admixtures and do not give any indication about cement-superplasticizer interaction.
3. Analysing cement mortars with equivalent composition to the concrete mixture is effective for detecting workability variations and cement-superplasticizer compatibility problems. Effects of aggregate on test results are minimised by using standardised sand. Besides, mortar tests are simple, easy to carry out and require smaller amounts of material than concrete tests.
4. Based on the obtained results, the mortar and paste flow tests and the centrifuge test are the most sensitive tests to detect the causes behind workability variations of SCC mixtures. The problem with cone flow tests is that they are not suitable for assessing pastes with low fluidity. Thus, the centrifuge test is a promising substitute test for the Marsh cone test with the advantage of being equally precise for lower and higher fluidity pastes.
5. Many factors influence fluidity and the hydration process of cement paste. Some of these factors may also have synergistic effects. This makes it difficult to point out one particular parameter which is responsible for producing a certain property. A more 'robust' measure of association between two variables, the Spearman's correlation coefficient, was recommended here instead of a classical correlation coefficient.
6. Quality information presently available from the cement supplier is not detailed enough. Physical and chemical parameters from cement characterization are necessary for explaining the variation of early age properties of SCC mixtures. Cement producers should control cement fineness, SO_3 level and forms of SO_3 present to produce stable cements for SCC workability.
7. As expected, it was found that empirical test results correlate with the rheological parameters of pastes, namely, yield stress and plastic viscosity. Furthermore, the existing models for predicting the mini-slump flow diameter and the flow time of pastes were implemented and compared with experimental data. A reasonable approximation was found between measured and predicted values, but a better approximation could be expected if the same protocol to determine yield stress (mixing sequence, test equipment, tool geometry, testing sequence) had been followed.
8. The target paste properties, for different fine aggregate content, can be defined in terms of both empirical test results and rheological parameters, linking mortar and paste properties that are adequate for SCC.

Acknowledgments

This research was financed by FCT – Portuguese Foundation for Science and Technology POCTI/ECM/61649/2004 and research projects PTDC/ECM/70693/2006 and supported by FCT Research Grant SFRH/BD/25552/2005. Collaboration and materials supplied by CIMPOR, SIKA and COMITAL is also gratefully acknowledged. We are grateful to the anonymous referees for their helpful comments and suggestions.

References

- [1] Ferraris CF, Olla KH, Hill R. The influence of mineral admixtures on the rheology of cement paste and concrete. *Cem Concr Res* 2001;31(2):245–55.
- [2] Martys N, Ferraris CF. Simulation of SCC flow. In: Shah SP, editor. Proceedings of 1st North American conference on the design and use of self-consolidating concrete. Illinois: ACBM; 2002. p. 21–6.
- [3] Sakai E, Yamada K, Ohta A. Molecular structure and dispersion-adsorption mechanisms of comb-type superplasticizers used in Japan. *J Adv Concr Technol* 2003;1(1):16–25.
- [4] Flatt RJ. Interparticle forces and superplasticizers in cement suspensions. Phd thesis, Switzerland: École Polytechnique Fédérale de Lausanne; 1999.
- [5] Flatt RJ, Houst YF. A simplified view on chemical effects perturbing the action of superplasticizers. *Cem Concr Res* 2001;31(8):1169–76.
- [6] Yamada K, Sugamata T, Nakanishi H. Fluidity performances of evaluation of cement and superplasticizer. *J Adv Concr Technol* 2006;4(2):241–9.
- [7] BIBM, CEMBUREAU, EFCA, EFNARC, ERMCO. The European guidelines for self-compacting concrete. Specification, production and use; 2005.
- [8] Juvas K, Käppi A, Salo K, Nordenswan E. The effects of cement variations on concrete workability. Nordic Concrete Research, Publication no 26.
- [9] Wallevik OH, Kubens S, Müller F. Influence of cement-admixture interaction on the stability of production properties of SCC. In: Schutter GD, Boel V, editors. Proceedings of 5th international RILEM symposium on self-compacting concrete-SCC2007, vol. 1. Ghent: RILEM Publications S.A.R.L.; 2007. p. 211–6.
- [10] Kubens S, Wallevik O. Interaction of cement and admixtures – the influence of cement deliveries on rheological properties. In: Proceedings of the 16th iBausil, Weimar, Germany, 2006. p. 1_0679–86.
- [11] Aitcin PC, Jiang S, Kim BG. Cement/superplasticizer interaction. The case of polysulfonates. *Bull des Lab des Ponts et Chaussées* 2001;233:89–99.
- [12] Dransfield J. Admixtures for concrete, mortar and grout. In: Newman J, Choo BS, editors. Advanced concrete technology: constituent materials, vol. 1. Oxford: Elsevier; 2003.
- [13] Nunes S, Milheiro Oliveira P, Sousa Coutinho J, Figueiras J. Interaction diagrams to assess SCC mortars for different cement types. *Constr Build Mater* 2009;23:1401–12.
- [14] Okamura H, Ozawa K, Ouchi M. Self-compacting concrete. *Struct Concr* 2000;1:3–17.
- [15] Gomes P. Optimization and characterization of high-strength self-compacting concrete. Phd thesis, Barcelona: Universitat Politècnica de Catalunya; 2002.
- [16] Roussel N, Le Roy R. The Marsh cone: a test or a rheological apparatus. *Cem Concr Res* 2005;35(5):823–30.
- [17] Chhabra R, Richardson J. Non-newtonian flow in the process industries. Fundamentals and engineering applications. Oxford: Butterworth-Heinemann; 1999.
- [18] A basic introduction to rheology. Bohlin Instruments Ltd.; 1994.
- [19] Yahia A, Khayat KH. Analytical models for estimating yield stress of high-performance pseudoplastic grout. *Cem Concr Res* 2001;31(5):731–8.
- [20] Grünwald S. Performance-based design of self-compacting fibre reinforced concrete. Phd thesis, The Netherlands: Delft University of Technology; 2004.
- [21] Sprent P. Applied nonparametric statistical methods. London: Chapman & Hall; 1996.
- [22] Hanehara S, Yamada K. Interaction between cement and chemical admixture from the point of cement hydration, absorption behaviour of admixture, and paste rheology. *Cem Concr Res* 1999;29(8):1159–65.
- [23] Grünwald S, Walraven JC. Self-compacting concrete with viscosity agents in the fresh state. Technical report, Delft University of Technology; 2005.
- [24] Roy RL, Roussel N. The Marsh cone as a viscometer. Theoretical analysis and practical limits. *Mater Struct* 2005;38(1):25–30.
- [25] Flatt RJ, Larosa D, Roussel N. Linking yield stress measurements. Spread test versus Viskomat. *Cem Concr Res* 2006;36(1):99–109.
- [26] Roussel N, Coussot P. "Fifty-cent rheometer" for yield stress measurements. From slump to spreading flow. *J Rheol* 2005;49(3):705–18.
- [27] Saak AW, Jennings HM, Shah SP. A generalized approach for the determination of yield stress by slump and slump flow. *Cem Concr Res* 2004;34(3):363–71.
- [28] Roussel N, Stefani C, Leroy R. From mini-cone test to Abrams cone test. Measurement of cement-based materials yield stress using slump tests. *Cem Concr Res* 2005;35(5):817–22.
- [29] Saak AW. Characterization and modelling of the rheology of cement paste. With applications toward self-flowing materials. Phd thesis. Illinois: Northwestern University; 2000.